Exchange interactions in $Cd_{1-x}Mn_xTe$ wide quantum wells

C. Rice, L. C. Smith, J. J. Davies,* and D. Wolverson
Department of Physics, University of Bath, Bath, BA2 7AY, United Kingdom

M. Wiater, G. Karczewski, and T. Wojtowicz
Institute of Physics, Polish Academy of Sciences, Warsaw, Poland
(Received 29 August 2012; published 24 October 2012)

The exchange interactions between excitons and manganese ions in wide (80 nm) quantum wells of $Cd_{1-x}Mn_xTe$ ($x \approx 0.0015$ and $x \approx 0.00027$) have been measured for states with center of mass quantum numbers up to 10. The corresponding translational wave vectors are in the range up to 4×10^6 cm^{-1} and in this range we detect no systematic variation of the exchange parameter $N_0(\alpha - \beta)$, which remains constant to within $\pm 3\%$. The result is consistent with previous studies of the wave vector dependence of the electron contribution $N_0\alpha$ but differs from previous observations of the wave vector dependence of exciton exchange interaction in quantum wells with much higher concentrations of manganese.

DOI: 10.1103/PhysRevB.86.155318 PACS number(s): 75.50.Pp, 71.35.Ji, 71.70.Gm, 75.30.Et

I. INTRODUCTION

Magnetic semiconductors are characterized by the very large exchange interactions between the charge carriers and the magnetic ions.[1] The consequent properties, notably the spin-dependent band gaps, lead to the possibility of structures such as spin injectors for a special class of electronic devices (e.g., Refs. 2–4). Such devices often involve features at the nanoscale and it therefore becomes important to investigate the extent to which the magnetic properties of the charge carriers are changed under conditions where quantum confinement begins to occur.

As the spatial dimensions of the confining potential are reduced, the wave vectors of the confined particles increase. The consequent changes in the exchange interactions between the manganese ions and the charge carriers have been investigated both experimentally and theoretically in several studies[5–7] of $Cd_{1-x}Mn_xTe$ quantum wells of different widths. Measurements of the magnetic-field-induced splittings of excitonic transitions[5] imply reductions in the exciton-manganese exchange interactions of several percent in quantum wells of width 4.5 nm: the reduction was greater than originally predicted from the theory of Ref. 6, which deals only with that part of the interaction due to electrons. In a later study, by electron spin-flip Raman (SFR) scattering, in wells of this width[7] reductions in the *electron*-manganese exchange interaction of up to 10 percent were observed and attributed to a switching on of kinetic contributions to the interaction that are forbidden at zero wave vector. Inclusion of these contributions improves the agreement with the experimental data of Ref. 5. However, a different interpretation of the data has been proposed in Ref. 8, pointing to the need for further studies, particularly since knowledge of the behavior of the exchange interactions under quantum confinement is fundamental to the understanding of quantum structures that contain magnetic ions (e.g., Ref. 9).

In the present paper we describe a different approach, based on the study of excitons in very wide quantum wells. In such wells the excitons can be described in the center of mass (CoM) approximation. Provided that the well depths are sufficiently deep, the component of the CoM translational wave vector in the growth direction (K_z) becomes quantized according to $K_z = N\pi/L$, where L is the width of the well and $N = 1,2,3,\ldots$. The exciton recombination energies now depend on N and, in specimens of sufficient quality, can be resolved individually in photoluminescence or reflectivity spectra. The exchange energies and Zeeman splitting in a magnetic field associated with each value of N (and hence with each value of the the wave vector) can then be determined, all in one quantum well. Furthermore, the penetration of the exciton wave function into the barrier materials is small, so that interface effects are unimportant. In the case of quantum wells that contain no magnetic ions, the approach has already been used to show that the Zeeman splitting of excitons (characterized by the g values) depends strongly on the translational wave vector and the behavior has been shown to be due to mixing between the heavy-hole exciton ground state (of $1S$ character) and higher-lying P-like *light*-hole exciton states.[10–14] In wells that contain magnetic ions, this mixing will also be present and its effect on the exchange interaction must also be taken into account, in addition to the mechanisms considered previously.

The plan of the paper is as follows. In Sec. II we describe the samples studied, followed by descriptions of the reflectivity and photoluminescence spectra (Sec. III) and of the spin-flip Raman (SFR) spectra (Sec. IV). Discussion of the exchange parameters and the gyromagnetic ratios (g values) as functions of wave vector (Sec. V) is followed by our conclusion.

II. SAMPLE DETAILS

Two wide quantum well samples were grown by molecular beam epitaxy on GaAs substrates, with $Cd_{1-y}Mg_yTe$ barriers ($y \sim 0.3$) and an 800 Å $Cd_{1-x}Mn_xTe$ well, where $x \sim 0.00146$ for Sample A and $x \sim 0.00027$ for Sample B (as determined from reflectivity experiments, see Sec. III). The difference in band gaps between the well and barrier materials is therefore of the order of 480 meV. The strain in these quantum wells is expected to be similar to that observed in several similar structures that contain no manganese and is expected to cause the heavy-hole (HH) valence band to lie at about 15 meV lower in energy than the light-hole (LH) band, so that the

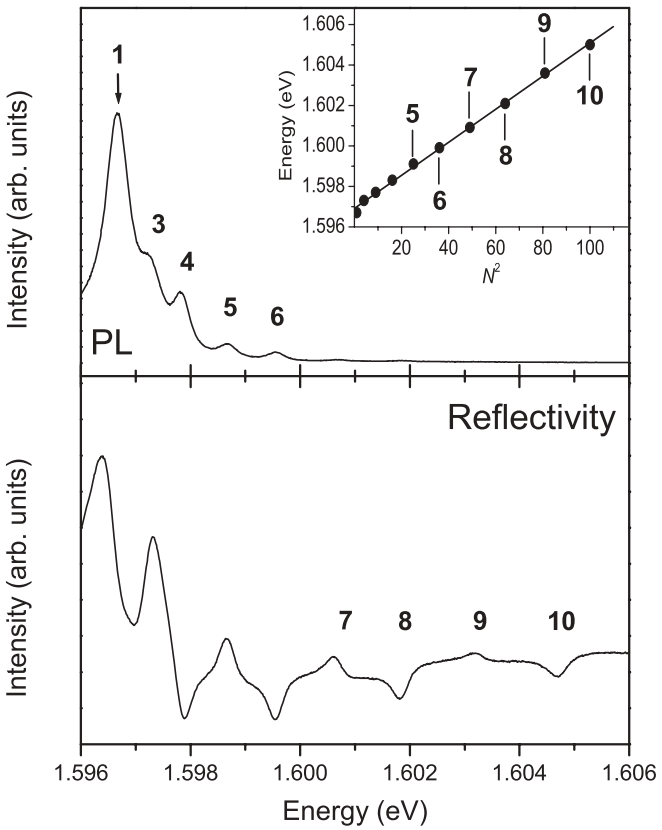

FIG. 1. PL (top) and reflectivity (bottom) spectra for Sample A, taken in zero magnetic field at 1.4 K. The values of the quantization index N are shown. The inset shows how the transition energies depend on N^2, giving the expected straight line with gradient corresponding to a translational mass $M = 0.72m_0$.

lowest-lying exciton states involve the heavy holes (as for example, in Refs. 10–14).

III. REFLECTIVITY AND PHOTOLUMINESCENCE SPECTRA

Photoluminescence (PL), reflectivity, and Raman scattering spectra were recorded with the samples immersed in a superfluid helium at $T = 1.4$ K with magnetic fields of up to 6 Tesla applied along the sample growth direction (taken to be the z axis). The PL and Raman spectra were obtained with a tuneable CW Ti-sapphire laser and the reflectivity with a tungsten filament lamp. The spectra were recorded by using a triple grating spectrometer with cooled CCD detection.

PL and reflectivity spectra in zero magnetic field from sample A are shown in Fig. 1. To a good approximation, the transition energies are given by

$$E_N = E_0 + \frac{N^2h^2}{8M_{\rm HH}L^2}, \tag{1}$$

where $M_{\rm HH}$ is the exciton translational mass for motion in the growth direction, and E_0 is the exciton transition energy for a well of infinite width.[15,16] The inset shows the expected linear dependence of energy on the square of the quantization index N and gives $M_{\rm HH} = 0.72m_0$. This agrees well with the expected value of $M = m_e + m_{\rm HH} = 0.09m_o + 0.59m_o$

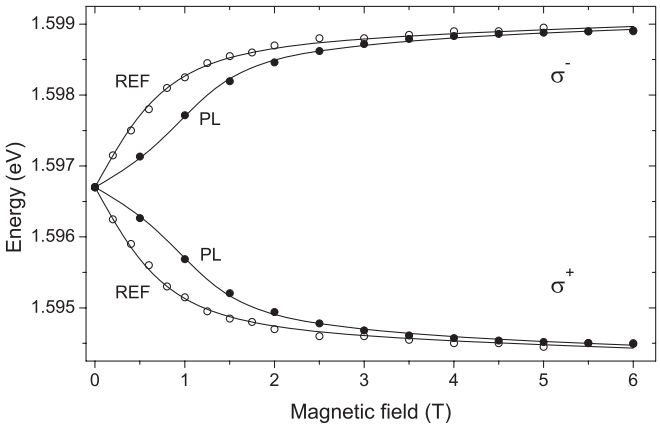

FIG. 2. PL and reflectivity signal energies as functions of magnetic field for the $N = 1$ transition in Sample A. The diamagnetic contributions have been removed so that the shifts in energy are symmetric about the starting point in zero field. The upper and lower branches correspond respectively to σ^- and σ^+ transitions. As the excitation power is reduced, the PL data (filled circles) points move towards those from the reflectivity spectra (open circles). The continuous lines are calculated as discussed in the text.

(Ref. 17). The spectra in zero field for Sample B are similar to those for Sample A, but shifted to lower energies by about 1.8 meV as a result of the lower concentration of manganese.

When a magnetic field is applied in the growth direction, the transitions split into pairs with opposite senses of circular polarization. Each pair corresponds to the allowed optical transitions from the heavy-hole exciton states $|m_J = 3/2, m_s = -1/2\rangle$ and $|m_J = -3/2, m_s = 1/2\rangle$, where m_J and m_s are the magnetic quantum numbers of the heavy-hole and electron respectively. Examples of the behavior are shown in Fig. 2 for the $N = 1$ transition for Sample A. As the excitation power is reduced, the PL energies approach increasingly the reflectivity energies. The complete fan diagrams are shown in Figs. 3 and 4.

This marked difference between the PL and reflectivity fan diagrams (Fig. 2) has been attributed[18] to energy transfer between the excitons and the Mn^{2+} spin system through a spin-flip scattering process mediated by the presence of a 2DEG in the quantum well or by the photo-excited carriers themselves.[19,20] The effect is predicted to be particularly marked at low manganese concentrations (x less than about 0.05) and can be modeled[18] by describing the Mn^{2+} spin system empirically with a field-dependent spin temperature given by $T(B) = T_a + T_b \exp(-B^2/\gamma)$. In Fig. 2 this scheme has been used to fit the data for the $N = 1$ peak in Sample A with the values $T_a = 2.0$ K, $T_b = 2.5$ K, and $\gamma = 1.0$ T^2. However, because of the need to correct for these heating effects in the PL, it is the reflectivity spectra that we have used for analysis.

For a particular value of N the transition energies in the reflectivity spectra are expected to be given by

$$E = E_N \pm \tfrac{1}{2}g_{\rm exc}\mu_B B \mp \tfrac{1}{2}N_0(\alpha - \beta)\overline{x}SB_S(y) + D(N)B^2. \tag{2}$$

Here $g_{\rm exc}$ is the g value of the exciton and for fields along z takes the form[11]

$$g_{\rm exc} = g_{\rm HH} - g_e + g(K_z), \tag{3}$$

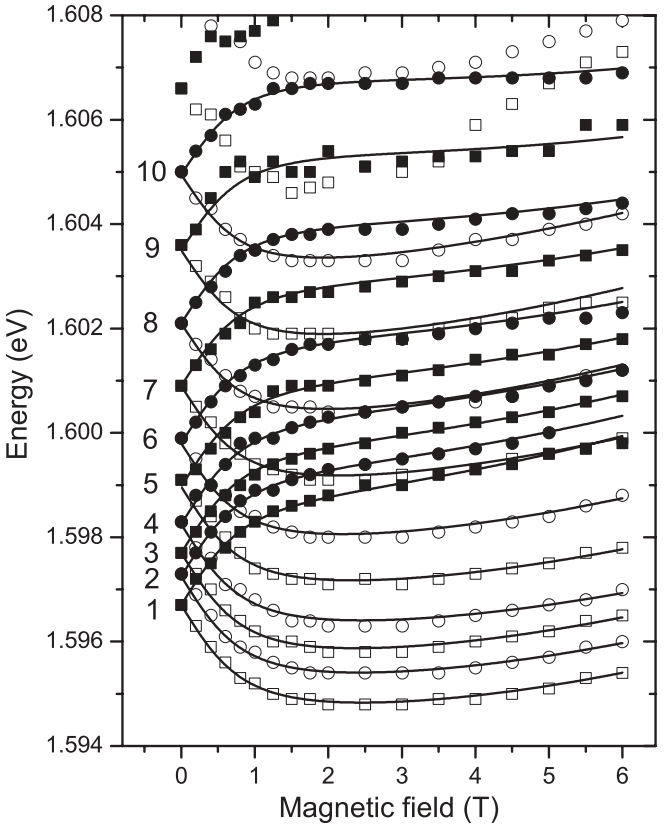

FIG. 3. Reflectivity transition energies at 1.4 K for excitons in Sample A. Filled symbols denote σ^- polarization and open circles σ^+. The transitions are labeled with the quantization index numbers N. Odd and even transitions are represented by squares and circles respectively. Transitions with $N > 10$ have not been fitted because of overlap with Landau level transitions. Continuous curves are of the form of Eq. (2), with $N_0(\alpha - \beta)$ kept constant at 1.11 eV and $\overline{x} = 0.00146$. The values of the exciton g value $g_{\rm exc}$ vary with N as shown in Fig. 5 and as discussed in Sec. V A.

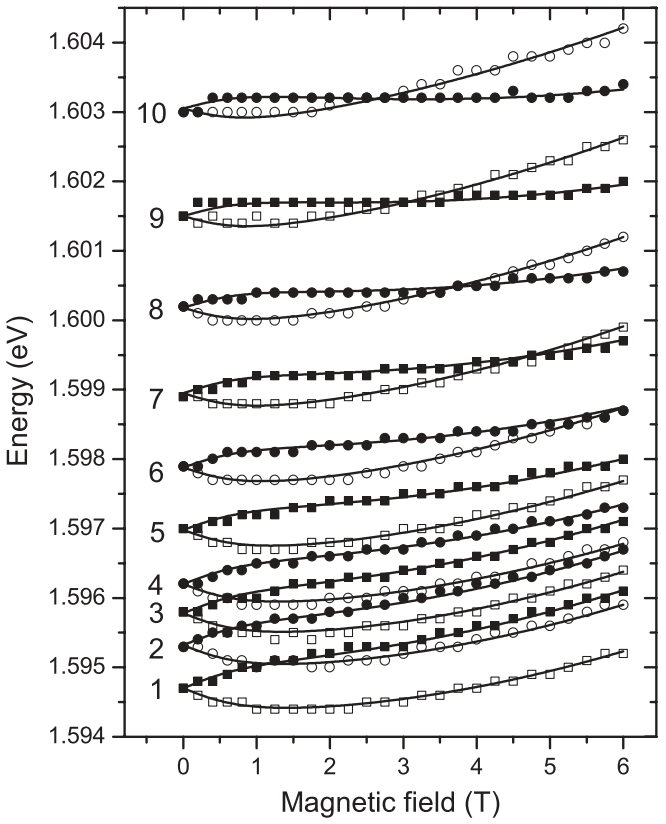

FIG. 4. Reflectivity transition energies at 1.4 K for excitons in Sample B. The symbols are as in Fig. 3. Continuous curves are of the form of Eq. (2), with $N_0(\alpha - \beta)$ kept constant at 1.11 eV and $\overline{x} = 0.00027$. The marked differences in behavior of the pairs of lines for different values of N is due to the rapidly changing values of $g_{\rm exc}$ (see Fig. 5 and Sec. V A) and is more noticeable than for Sample A because the exchange effects are now smaller.

where $g_{\rm HH}$ and g_e are the heavy-hole and electron g factors, respectively. The contribution $g(K_z)$, arises from motion induced mixing: it is a strong function of wave vector and depends strongly on the index N. Its origin is discussed in detail in Ref. 11.

The effect of the exchange interactions with the manganese ions is represented[21] by the third term in Eq. (2). At the present low manganese contents, the effective concentration of Mn^{2+} ions $\overline{x}$ is equal to x. The terms[21] $N_0\alpha = 0.22$ eV and $N_0\beta = -0.88$ eV characterize the exchange interactions between the manganese ions and the conduction and valence band states respectively and $B_S(u)$ is the Brillouin function for a spin $S = 5/2$, with $u = g_{\rm Mn}\mu_B/k_BT_{\rm eff}$. For the reflectivity $T_{\rm eff}$ is taken to be equal to the bath temperature of 1.4 K.

The final term in Eq. (2) represents the diamagnetic shifts. This term also is wave vector dependent and hence the parameter $D(N)$ is a strong function of N, as discussed in Ref. 11.

The continuous curves shown in Figs. 3 and 4 are calculated by using Eq. (2). For a particular value of N, the difference between the σ_+ and σ_- energies at a particular field depends on $g_{\rm exc}$ and on $\overline{x}N_0(\alpha - \beta)$. As B is increased from zero, the sensitivity to the exact value of $g_{\rm exc}$ is at first relatively small, becoming significant only as the effects of the exchange interactions begin to saturate: the determination of $g_{\rm exc}$ itself for each value of N thus depends sensitively on the high field data (this point is discussed further in Sec. V A). For Sample A, the data can be fitted accurately under the assumption that $N_0(\alpha - \beta)$ remains constant to within 3 percent over the range of wave vectors studied. In contrast, $g_{\rm exc}$ is found to change significantly with N, as shown in Fig. 5. For Sample B, $N_0(\alpha - \beta)$ is found to be constant to within 4% while $g_{\rm exc}$ varies as shown also in Fig. 5.

We note that in analyzing our data we have assumed a simple uncoupled excitonic dispersion and neglected effects from a coupled exciton-photon (polariton) system. This is a valid assumption given that the smallest K_z values for which we can observe splittings are well above the region where exciton-photon interaction is strong (see, e.g., Ref. 16).

IV. SPIN-FLIP RAMAN SPECTRA

Spin-flip Raman energy shifts for the two specimens are shown in Fig. 6. To within the experimental accuracy the shifts $\Delta E_{\rm SF}$ are independent of the direction of the magnetic field. Those labeled SFR are attributed to spin-flip transitions of

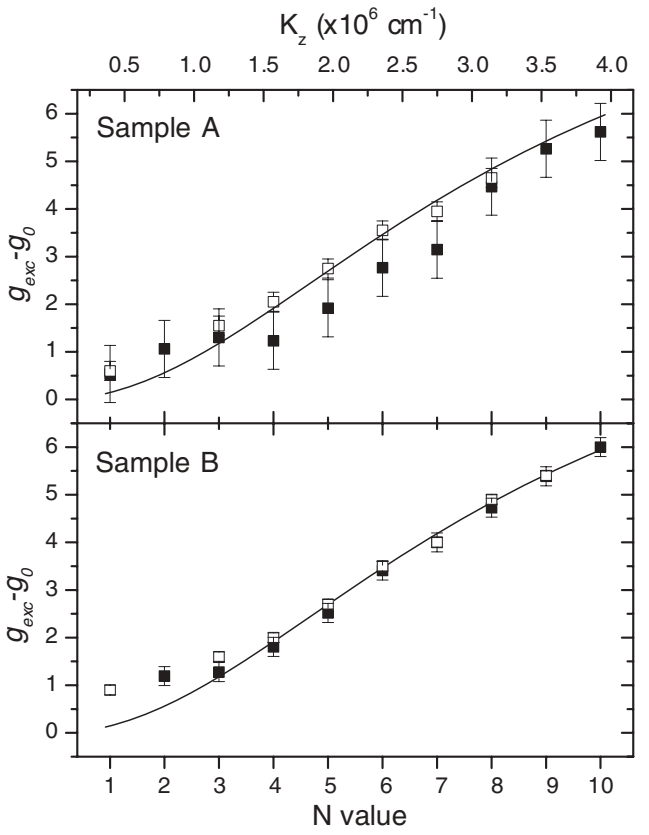

FIG. 5. Values of $(g_{\rm exc} - g_0)$ as a function of the translational quantum number N. Results from reflectivity data are shown in solid squares, while open squares denote PL measurements. For Sample A (top) a value of $g_0 = -2.1$ has been used, and for Sample B (bottom) $g_0 = -1.3$. The continuous curves are the prediction of the model of Ref. 11 with the strain-induced energy splitting between the LH and HH valence bands taken to be 15 meV.

electrons in the quantum wells, possibly bound at shallow donors or by other potential fluctuations, so that

$$\Delta E_{\rm SF} = g_e \mu_B B + \overline{x} N_0 \alpha S B_S(u). \qquad (4)$$

Using this equation and with $N_0\alpha$ taken to be 0.22 eV, we find that for sample A, $\overline{x} = 0.00186 \pm 0.00002$ and $g_e = -1.9 \pm 0.1$, while for sample B, $\overline{x} = 0.00025 \pm 0.00002$ and $g_e = -1.6 \pm 0.1$. The reported g values for conduction band electrons in CdTe are in the range -1.59 to -1.68, according to the state of binding (see Ref. 22 for a summary). The value of g_e measured for Sample A therefore appears unusually high and is discussed further in Sec. V A. The points labeled PMR are due to paramagnetic resonance excitations of manganese ions and correspond to a g value $g_{\rm Mn} = 2.00$.

V. DISCUSSION

A. *g* values

For convenience, we discuss first the values of $g_{\rm exc}$. Studies of spectra from nonmagnetic wells show that the contribution $g(K_Z)$ [see Eq. (3)] is a strong function of the z component K_Z of the exciton translational wave vector. The dependence is a result of mixing between the $1S$ heavy-hole exciton ground state and excited exciton nP states of light-hole character (and

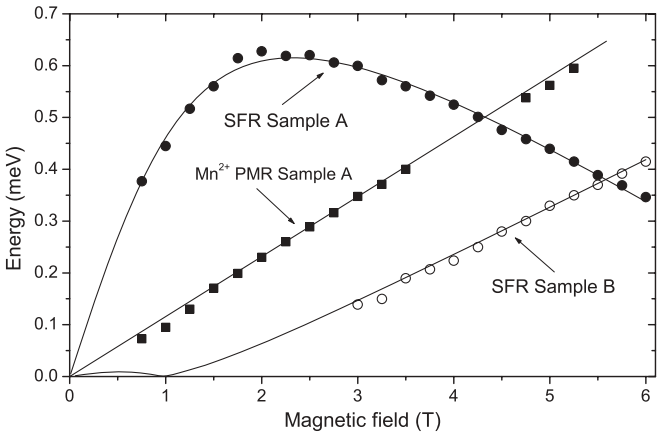

FIG. 6. SFR energy magnitudes as functions of magnetic field. Solid symbols are for Sample A, open symbols for Sample B. Circles and squares represent electron spin-flip and manganese spin-flip energies respectively. The continuous lines are calculated with $N_0\alpha = -0.22$ eV and with $\overline{x} = 0.00186$, $g_e = -1.9$, $T = 2.4$ K (Sample A) and $\overline{x} = 0.00025$, $g_e =$ -1.6, $T = 2.4$ K (Sample B). For the Mn^{2+} PMR energy, $g_{\rm Mn} = 2.00$.

is therefore strain dependent). For (001) quantum wells, the mixing is due to the γ_3 term that appears in the Luttinger Hamiltonian[23] that describes the valence band. Details of the mechanism are discussed in Ref. 11. Excellent agreement between the predicted and experimental values of $g(K_z)$ is obtained, not only for CdTe,[11,13] but also for ZnSe[12] and ZnTe.[14] In the present study, the manganese concentrations in the well are very low, so the parameters used to calculate $g(K_Z)$ are taken to be the same as for CdTe. Equation (3) can be rewritten as $g_{\rm exc} = g_o + g(K_Z)$, where g_o is the exciton g value for notional zero wave vector. In Fig. 5 we show the calculated dependencies of $g_{\rm exc}$ on K_z for a strain splitting between the light and heavy-hole valence bands of 15 meV and for values of $g_0 = -2.1$ and $g_0 = -1.3$ for Samples A and B respectively. The *changes* in $g_{\rm exc}$ as K_z increases are in good agreement with prediction. There is, however, an unexpected difference between g_o for the present specimens and the value of $g_o = -0.75$ found for otherwise identical but nonmagnetic CdTe wells.[11] There is evidence that g_o is strain dependent[11,13] but this cannot account for the present difference.

For Sample A, there therefore appears to be an additional contribution of $\delta g_{\rm exc} \approx -1.35$ to the exciton g value obtained from the reflectivity spectra and an additional contribution of $\delta g_e \approx -0.3$ to the electron g value found from the SFR measurements. In both cases, the g values were determined by using the high-field part of the fan diagrams under the assumption that the exchange contributions to the observed splittings are represented accurately by Brillouin functions (i.e., by assuming that the magnetism of the manganese ions that interact with the charge carriers is accurately described by such functions). If this is not the case, the determination of the g values will be in error and additional contributions to the energy shifts will appear which are proportional to the exchange interaction involved: in the case of exciton reflectivity this interaction depends on $N_0(\alpha - \beta)$ and in the case of the electron SFR spectra it depends on $N_0\alpha$. Thus, the contributions will be in the ratio of $|(\alpha - \beta)/\alpha| \approx 5$,

which compares with the ratio $\delta g_{\rm exc}/\delta g_e \approx 4.5$. It has often been assumed[1] that the effect of the carrier spins on the magnetization of the manganese ions can be neglected but recent studies[24–26] at manganese concentrations that are low suggest that this may not then be the case. This is particularly the case at the low concentrations used in the present experiments, since, in the case of Sample A, there is a crossover in energies between the electron and manganese spin-flip energies (see Fig. 6) in the region near 4 Tesla, so that the manganese spin system could become partly polarized through interaction with the electron spin system. This occurs at precisely the field range used for determining the g values. Consequent small changes in the slopes of the curves in Fig. 3 in this field region would lead to an apparent change in the value of g_0. Importantly, however, the change would be the same for all values of the quantization index N, so that the dependence of $(g_{\rm exc} - g_0)$ on K_z (Fig. 5) would be unaffected and would be as predicted by the model of Ref. 11.

B. Exchange parameters

In fitting the reflectivity data (Figs. 3 and 4), derivation of the exchange parameters (which depend on the saturation values of the energy splittings) is essentially independent of the derivation of the exciton g values (which depend on the slopes of the curves in the fan diagrams at high fields, as discussed in Sec. V A). We find no systematic variation in $\overline{x}N_0(\alpha - \beta)$ for either sample: we can fit the data by assuming that $N_0(\alpha - \beta)$ remains constant to within 3% for Sample A, to within 4% for Sample B and by using the values of $g_{\rm exc}$ that appear in Fig. 5. We thus deduce that for K_z up to 4×10^6 cm^{-1}, the exchange interaction between the HH excitons and Mn^{2+} ions does not change beyond these limits.

In addition to the possible effects on the exchange parameters discussed in Refs. 5–7, we also need to consider the effects (not previously considered) of the motion-induced mixing, which leads to the strong wave vector dependence of the exciton g values. The HH excitons with hole angular momentum components $m_J = \pm 3/2$ are mixed with LH excitons with $m_J = \pm 1/2$ (the electron angular momentum component is not changed) and for these LH excitons the exchange splitting is proportional to $N_0(\alpha - \beta/3)$, rather than to $N_0(\alpha - \beta)$, so that there is a corresponding reduction in the magnitude of the splitting. The change in magnitude as a function of wave vector can be found following the methods described in Ref. 11: with the Luttinger parameter $\gamma_3 = 1.9$ and the exciton Bohr radius $a_{\rm exc}$ taken to be 7.2 nm,[11] the calculated fractional reduction in the exciton energy splitting is shown in Fig. 7. The largest reduction occurs at an exciton translational wave vector of about 3×10^6 cm^{-1} and is of the order of 1%. This contribution is therefore comparable to the changes predicted using the mechanisms of Ref. 7, but lies beneath the accuracy of the present experiments.

C. Comparison between the reflectivity and spin-flip Raman data

For Sample A, the values of $\overline{x}$ obtained from the reflectivity ($\overline{x}_{\rm Ref} = 0.00146$) and SFR data ($\overline{x}_{\rm SFR} = 0.00186$) were calculated by using the reported values[21] of $N_0\alpha = 220 \pm 10$ meV and $N_0\beta = -880 \pm 40$ meV. We discount the possibility that the differences between these values of $\overline{x}$ are caused by macroscopic nonuniformity of the layers since the spectra were obtained from the same regions of the samples and since the reflectivity spectra are always sharp. If we write $\beta = p\alpha$, then the parameters $\overline{x}_{\rm Ref}N_0(\alpha - \beta)$ (obtained from the reflectivity) and $\overline{x}_{\rm SFR}N_0\alpha$ (obtained from the SFR data) are in the ratio $\overline{x}_{\rm Ref}(1 + p)/\overline{x}_{\rm SFR}$, which, by experiment equals 4.1 ± 0.3. For $\overline{x}_{\rm Ref}$ and $\overline{x}_{\rm SFR}$ to be equal, we require $p = 3.0 \pm 0.3$. This compares with the value of 4.0 ± 0.5 obtained from the accepted values,[21] which were obtained for specimens with much higher manganese concentrations. A possible explanation of the difference is that the specimens are nonuniform on the *microscopic* scale, with the SFR and reflectivity signals originating from different regions within this length scale. A further possibility is a concentration dependence of $N_0\alpha$ and/or $N_0\beta$. However, a firm conclusion requires further experiments.

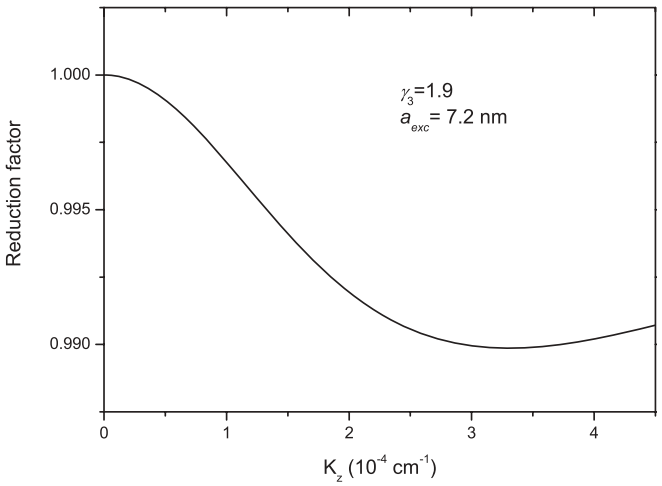

FIG. 7. The fractional reduction factor in the exchange splitting caused by the wave-vector-dependent mixing of the HH and LH exciton states as calculated by using the model of Ref. 11. The strain-induced energy splitting between the LH and HH valence bands is taken to be 15 meV.

VI. CONCLUSION

We have studied excitons with translational wave vectors K_z up to 4×10^6 cm^{-1} in wide diluted magnetic semiconductor quantum wells of $Cd_xMn_{1-x}Te$. We find no systematic dependence of the exciton-manganese exchange interaction with wave vector and find that $N_0(\alpha - \beta)$ remains constant to within 3% over this range. A translational wave vector of 4×10^6 cm^{-1} corresponds to the value of K_z for the $N = 1$ confined state of an exciton in a deep well of width $L \approx 8$ nm. For wells of such width, the SFR studies of Ref. 7 indicate that $N_0\alpha$ has decreased by about 10%; since $N_0\alpha$ contributes only a fifth of the exciton exchange interaction, such a decrease would lie beyond our experimental accuracy. In contrast, the PL studies of Ref. 5 show apparent decreases in $N_0(\alpha - \beta)$ of about 7% for such a well width and such a change would

have been observable in our samples. The reasons for this difference are not clear, but may be related to the much lower manganese concentrations that we have used. The advantage of low concentrations is that complications caused by pairing between the manganese ions are eliminated: as discussed in Ref. 8, such complications may lead to apparent reductions in the exchange splittings and would not occur in the present samples.

ACKNOWLEDGMENTS

We are grateful to the Engineering and Physical Sciences Research Council (UK) for support of this work (Project No. EP/E025412) and for support through a research studentship to C.R. The research in Poland was partially supported by the European Union within the European Regional Development Fund, through grant Innovative Economy (POIG.01.01.02-00-008/08).

*j.j.davies@bath.ac.uk

[1] J. K. Furdyna, J. Appl. Phys. **64**, R29 (1988).

[2] R. Fiederling, M. Keim, G. Reuscher, W. Ossau, G. Schmidt, A. Waag, and L. W. Molenkamp, Nature (London) **402**, 787 (1999).

[3] G. Schmidt, R. Fiederling, M. Keim, G. Reuscher, T. Gruber, W. Ossau, A. Waag, and L. W. Molenkamp, Superlattices Microstruct. **27**, 297 (2000).

[4] C. Gould, G. Schmidt, G. Richter, R. Fiederling, P. Grabs, and L. W. Molenkamp, Appl. Surf. Sci. **190**, 395 (2002).

[5] G. Mackh, W. Ossau, A. Waag, and G. Landwehr, Phys. Rev. B **54**, R5227 (1996).

[6] A. K. Bhattacharjee, Phys. Rev. B **58**, 15660 (1998).

[7] I. A. Merkulov, D. R. Yakovlev, A. Keller, W. Ossau, J. Geurts, A. Waag, G. Landwehr, G. Karczewski, T. Wojtowicz, and J. Kossut, Phys. Rev. Lett. **83**, 1431 (1999).

[8] H. Bednarski, J. Cisowski, and J. C. Portal, J. Cryst. Growth **184-185**, 996 (1998).

[9] L. Besombes, Y. Léger, L. Maingault, D. Ferrand, H. Mariette, and J. Cibert, Phys. Rev. Lett. **93**, 207403 (2004).

[10] J. J. Davies, D. Wolverson, V. P. Kochereshko, A. V. Platonov, R. T. Cox, J. Cibert, H. Mariette, C. Bodin, C. Gourgon, E. V. Ubyivovk, Yu. P. Efimov and S. A. Eliseev, Phys. Rev. Lett. **97**, 187403 (2006).

[11] L. C. Smith, J. J. Davies, D. Wolverson, S. Crampin, R. T. Cox, J. Cibert, H. Mariette, V. P. Kochereshko, M. Wiater, G. Karczewski, and T. Wojtowicz, Phys. Rev. B **78**, 085204 (2008).

[12] J. J. Davies, L. C. Smith, D. Wolverson, A. Gust, C. Kruse, D. Hommel, and V. P. Kochereshko, Phys. Rev. B **81**, 085208 (2010).

[13] J. J. Davies, L. C. Smith, D. Wolverson, V. P. Kochereshko, J. Cibert, H. Mariette, H. Boukari, M. Wiater, G. Karczewski, T. Wojtowicz, A. Gust, C. Kruse, and D. Hommel, Phys. Status Solidi B **247**, 1521 (2010).

[14] L. C. Smith, J. J. Davies, D. Wolverson, H. Boukari, H. Mariette, V. P. Kochereshko, and R. T. Phillips, Phys. Rev. B **83**, 155206 (2011).

[15] Y. Merle d'Aubigné, Le Si Dang, A. Wasiela, F. d'Albo, and A. Million, J. Phys. (Paris) **48**, C5-363 (1987).

[16] H. Tuffigo, R. T. Cox, N. Magnea, Y. Merle d'Aubigné, and A. Million, Phys. Rev. B **37**, 4310 (1988).

[17] Le Si Dang, G. Neu, and R. Romestain, Solid State Commun. **44**, 1187 (1982).

[18] B. König, I. A. Merkulov, D. R. Yakovlev, W. Ossau, S. M. Ryabchenko, M. Kutrowski, T. Wojtowicz, G. Karczewski, and J. Kossut, Phys. Rev. B **61**, 16870 (2000).

[19] D. Keller, D. R. Yakovlev, B. König, W. Ossau, Th. Gruber, A. Waag, L. W. Molenkamp, and A. V. Scherbakov, Phys. Rev. B **65**, 035313 (2001).

[20] A. V. Koudinov, Yu. G. Kusrayev, and I. G. Aksyanov, Phys. Rev. B **68**, 085315 (2003).

[21] J. A. Gaj, R. Planel, and G. Fishman, Solid State Commun. **29**, 435 (1979).

[22] S. Tsoi, I. Miotkowski, S. Rodriguez, A. K. Ramdas, H. Alawadhi, and T. M. Pekarek, Phys. Rev. B **69**, 035209 (2004).

[23] J. M. Luttinger, Phys. Rev. **102**, 1030 (1956).

[24] F. J. Teran, M. Potemski, D. K. Maude, D. Plantier, A. K. Hassan, A. Sachrajda, Z. Wilamowski, J. Jaroszynski, T. Wojtowicz, and G. Karczewski, Phys. Rev. Lett. **91**, 077201 (2003).

[25] T. Clément, D. Ferrand, L. Besombes, H. Boukari, and H. Mariette, Phys. Rev. B **81**, 155328 (2010).

[26] P. Barate, S. Cronenberger, M. Vladimirova, D. Scalbert, F. Perez, J. Gomez, B. Jusserand, H. Boukari, D. Ferrand, H. Mariette, J. Cibert, and M. Nawrocki, Phys. Rev. B **82**, 075306 (2010).